SAND REPORT

SAND2002-0100
Unlimited Release
Printed January 2002

The SEAWOLF Flume: Sediment Erosion Actuated by Wave Oscillations and Linear Flow

Richard Jepsen, Jesse Roberts, Joseph Z. Gailani, and S. Jarrell Smith

Prepared by
Sandia National Laboratories
Albuquerque, New Mexico 87185 and Livermore, California 94550

Sandia is a multiprogram laboratory operated by Sandia Corporation, a Lockheed Martin Company, for the United States Department of Energy under Contract DE-AC04-94AL85000.

Issued by Sandia National Laboratories, operated for the United States Department of Energy by Sandia Corporation.

Available to DOE and DOE contractors from
U.S. Department of Energy
Office of Scientific and Technical Information
P.O. Box 62
Oak Ridge, TN 37831

Telephone: (865)576-8401
Facsimile: (865)576-5728
E-Mail: reports@adonis.osti.gov
Online ordering: http://www.doe.gov/bridge

Available to the public from
U.S. Department of Commerce
National Technical Information Service
5285 Port Royal Rd
Springfield, VA 22161

Telephone: (800)553-6847
Facsimile: (703)605-6900
E-Mail: orders@ntis.fedworld.gov
Online order: http://www.ntis.gov/ordering.htm

SAND 2002-0100
Unlimited Release
Printed January 2002

The SEAWOLF Flume: Sediment Erosion Actuated by Wave Oscillations and Linear Flow

Richard Jepsen and Jesse Roberts
Carlsbad Programs Group
Soil and Sediment Transport Lab
Sandia National Laboratories
P.O. Box 5800
Albuquerque, NM 87185-1395

Joseph Z. Gailani and S. Jarrell Smith
U.S. Army Engineer Research and Development Center
Coastal and Hydraulics Laboratory
Vicksburg, MS 39180

Abstract

Sandia National Laboratories has previously developed a unidirectional High Shear Stress Sediment Erosion flume for the US Army Corps of Engineers, Coastal Hydraulics Laboratory. The flow regime for this flume has limited applicability to wave-dominated environments. A significant design modification to the existing flume allows oscillatory flow to be superimposed upon a unidirectional current. The new flume simulates high-shear stress erosion processes experienced in coastal waters where wave forcing dominates the system. Flow velocity measurements, and erosion experiments with known sediment samples were performed with the new flume. Also, preliminary computational flow models closely simulate experimental results and allow for a detailed assessment of the induced shear stresses at the sediment surface.

This work was supported by the U.S. Army Corps of Engineers under Contract No. W81EWFO1944045 Amend. #1

Acknowledgement

The authors would like to thank Scott James for his careful review and helpful suggestions regarding this report.

CONTENTS

FIGURES

TABLES

1.0 Introduction

Sandia National Laboratories (SNL) has designed, constructed, and tested a high-shear flume that superimposes an oscillatory flow upon a unidirectional current. The apparatus is named the Sediment Erosion Actuated by Wave Oscillations and Linear Flow (SEAWOLF) Flume. The SEAWOLF can be housed in a self-contained, mobile facility and used on site in research and mission support investigations of combined current and wave-induced erosion of in-situ contaminated sediment, dredged material mixtures composed of cohesive and non-cohesive sediments, or other sediments.

Previously, SNL built and operated a unidirectional high shear stress sediment erosion flume (SEDFlume, McNeil et al, 1996) for field and laboratory studies. The SEAWOLF is a significant design modification of the SEDFlume that maintains the ability to measure erosion and the variation of erosion with depth below the sediment-water interface for a wide range of shear stresses. However, the SEAWOLF further has the capability to analyze the impact of oscillatory flow on erosion rate. This capability remedies shortcomings of erosion rate algorithms developed from measurements under unidirectional flow when predicting erosion in wave-dominated environments.

Results from hydrodynamic modeling of SEAWOLF indicate oscillatory flow regimes in the SEAWOLF induce shear stresses up to 10 Pa, while those combined with unidirectional flows induce shear stresses over 12 Pa. Erosion experiments were performed under a range of unidirectional and oscillatory flow combinations. These experiments verified model predictions that for the same instantaneous flow rate, the undeveloped oscillatory flow shear stresses are much greater than those generated by fully developed, unidirectional flow. Finally, effective shear stresses are determined from

erosion tests with known sediment samples, making SEAWOLF a useful tool for predictive modeling.

2.0 Device Description

2.1 Design Concept

The SEAWOLF flume channel is similar to the channel and erosion test section of the SEDFlume (McNeil et al., 1996; Roberts and Jepsen, 2001; Jepsen et al., 2001). The straight, clear polycarbonate flume channel (Figure 2.1a) is 2 m long and has a false bottom at the center where a core sample extracted directly from the field site (or created in the laboratory) is placed. The core is moved upward by the operator such that the sediment surface (i.e., the sediment/water interface) is level with the bottom of the flume channel. There is also a sediment trap at each end of the flume channel to remove sediments from the system so the test section does not experience sediment laden water from previously eroded material.

In the SEAWOLF, flow in the test section is controlled by the head difference between tanks A and C (Figure 2.1a). Oscillatory flow is generated by two pistons attached at each end of the flume channel that work in tandem. The operator controls a mechanical jack so that the sediment surface is kept flush with the flume bottom as the sediments erode under the specified current and oscillatory flow conditions. Erosion rate at the specified conditions is defined as the upward movement of the core divided by the time duration of the experiment. Typically, less than 2 cm is eroded during each erosion test. The core is typically 40-80 cm in depth and therefore permits analysis of sediment erosion with depth below the initial sediment/water interface.

The SEAWOLF permits the operator to conduct erosion rate experiments for shear stresses ranging from 0.1 Pa up to 10 Pa for the oscillatory regime, 0.1 to 3 Pa for unidirectional flow, and over 12 Pa for the combined flow regimes. The SEAWOLF is also used to measure the critical shear stress necessary to initiate erosion.

Two piston/cylinder arrangements drive the oscillatory flow while the unidirectional flow is forced by a head difference between tanks at each end of the flume (Figure 2.1b). Water is pumped from Tank B to Tank A to maintain the desired head in Tank A. The head in Tank A is greater than the head in Tank C. This head difference, Δh, drives the unidirectional flow. To change the unidirectional flow rate, Δh can be adjusted between each erosion test. Both Tank A and Tank C overflow into Tank B to maintain constant Δh during an erosion test. A computer, stepper motor, and linear ball-screw arrangement control the piston strokes that govern the maximum velocity and period of the oscillatory flow. In addition, valves at each end of the channel connecting to Tank A or Tank C are used to control both the unidirectional flow rates and the backflow into the tanks from the oscillatory flow. Within the test section, unidirectional flow rates can range between 0 and 35 gpm and the oscillatory peak rates range between 0 and 39 gpm. Asymmetric waves can be created when the valves connecting the channel to the tanks are unequally adjusted to manipulate backflow from the piston forcing. Clearly, the SEAWOLF flume simulates a wide range of wave conditions and shear stresses at the sediment water interface.

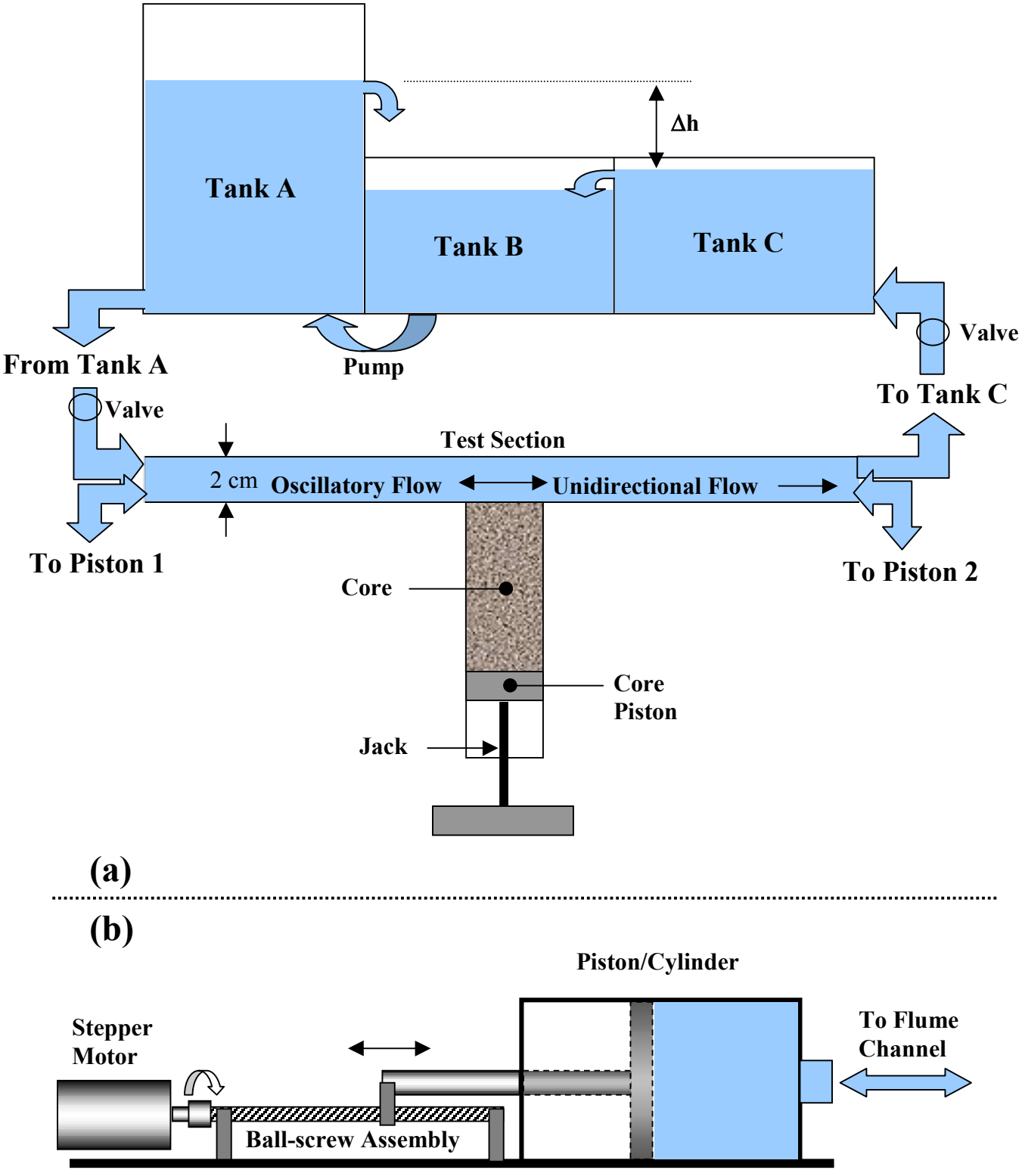

Figure 2.1: SEAWOLF Schematic:
(a) Channel, core, and tank assembly
(b) Motor, ball-screw, and piston assembly

2.2 Hydrodynamics

2.2.1 Internal Turbulent Flow

The relationship between internal turbulent flow and shear stress for a hydraulically smooth channel has been reported extensively for a unidirectional flume or internal channel (Schlichting, 1979, p.611; McNeil et al., 1996; Jepsen et al., 2001). The transcendental function relating the coefficient of resistance to system properties is

$$\frac{1}{\sqrt{\lambda}} = 2.0 \log\left(\frac{v_c d\sqrt{\lambda}}{\nu}\right) - 0.8 \quad , \tag{2.1}$$

ν = kinematic viscosity (m^2/s),
d = hydraulic diameter (m),
v_c = mean current flow velocity (m/s),
λ = coefficient of resistance (-).

The shear stress, τ (N/m^2), is included in the coefficient of resistance, λ, as follows

$$\lambda = \frac{8\tau}{\rho v_c} \quad , \tag{2.2}$$

ρ = water density (kg/m^3).

Equations (2.1) and (2.2) provide an implicit relationship for shear stress as a function of mean velocity.

The head difference, Δh, between Tanks A and C drives the velocity for the unidirectional flow in the channel. Unidirectional flow velocity is calculated from the Bernoulli equation:

$$\frac{P_A}{\rho} - \frac{v_c^2}{2} + g\Delta h = \frac{P_C}{\rho} + h_l, \tag{2.3}$$

g = gravity (m/s^2),
h_l = head losses (inlet, exit, channel, 90^o pipe bends) (m^2/s^2),
Δh= head difference (m),
$P_{A,C}$ = Pressure in Tanks A and C (N/m^2).

The pressures, P_A and P_C, are equal because both tanks are open to the atmosphere. Solving for v_c in equation (2.3) yields,

$$v_c = \sqrt{2g\Delta h - 2h_l} \qquad (2.4)$$

Head loss in the flume is estimated by accounting for flow rate, pipe diameter, pipe length, and pipe bends. For example, head difference of 0.45 m results in an approximate head loss of 4.0 m^2/s^2 and current velocity of 1 m/s when the valves to the tank (Figure 2.1a) are fully open. Partially closing the valves will increase the head loss. Valve adjustment offers fine control of the unidirectional flow rates. Although it is possible to calculate the head loss, it is not necessary for regular operation of the flume. The flow meter provides all relevant flow information and this calculation was performed only for design purposes.

2.2.2 Oscillatory Flow

The pistons attached to the ends of the channel drive the oscillatory flow in the channel. The sediment test section in the channel experiences the equivalent of one piston stroke volume across its surface with each piston stroke. The cross-sectional area of the piston arrangement is ~500 cm^2 and that of the channel is ~20 cm^2. The velocity in the channel from the oscillating piston is calculated from conservation of mass principles:

$$A_p V_p = A_c V_c , \qquad (2.5)$$

A_p = cross-sectional area of piston (m^2),
A_c = Cross-sectional area of channel (m^2),
V_p = velocity of piston(s) (m/s),
V_c = channel velocity (m/s).

This yields,

$$V_c = 25 V_p, \qquad (2.6)$$

when $A_p/A_c = 25$.

When the two pistons are 180^o out of phase, they aid each other (one piston is pushing and the other is pulling) and provide a preferential pathway for the flow through the channel and test section rather than forcing flow into the Tank A or C. Therefore, velocity over the test section (between the two pistons) is:

$$V_{\text{testsection}} = V_c \qquad (2.7)$$

Piston velocities are controlled by the stepper motor and range from 0 to 0.048 m/s. Therefore, oscillating velocities in the test section with no superimposed unidirectional current are between –1.2 and 1.2 m/s.

A constant, superimposed, unidirectional current is possible because the head difference between Tanks A and C is kept constant. The oscillatory forcing by the pistons does not affect the forcing of the superimposed unidirectional current because Tank A and C are open to the atmosphere and always free to spill excess water into the central reservoir of Tank B. A unidirectional pump driven current would not allow a reversal of flow direction or maintain a constant unidirectional forcing because the pump performance is dependent on the downstream head. Ultimately, a constant, superimposed

unidirectional flow can only be maintained by constant Δh achieved by the design shown in Figure 2.1a.

Oscillatory flow regimes are never fully developed. Furthermore, shear stresses are higher than those predicted by the fully developed assumptions, due to the larger velocity gradient in the boundary layer during developing flows (Schlicting, 1979, Chapter XV). Because the oscillatory flow is also time dependent, numerical modeling is most appropriate for determining the shear stress time history. The model for calculating shear stress will be discussed in Section 3.1. Maximum shear stress for the associated undeveloped oscillatory flow conditions (1.2 m/s) in SEAWOLF is 10 Pa.

In addition to the applied shear stresses, there is also a need to simulate a variety of wave shapes and periods. For each piston, the piston velocity is

$$V_p(t) = \frac{L\pi}{T}\sin(\omega t), \qquad (2.8)$$

where: L = stroke length (up to 0.4 m),
T = wave period (s),
ω= angular velocity (2π/T) (radians/s),
t = time (s).

This yields a sinusoidally varying flow velocity over the test section of

$$V_c = \frac{L\pi}{T}\left(\frac{A_p}{A_c}\right)\sin(\omega t), \qquad (2.9)$$

The amplitude of the wave and maximum piston velocity, V_p, is Lπ/T for equation (2.8). Since the maximum piston velocity, V_p, is 0.048 m/s (V_c = 1.2 m/s), the associated maximum wave period, T, for a 0.4 m maximum stroke length, L, is 26 s.

By linear wave theory, an estimate of the horizontal, bottom orbital velocities for a given wave height, wave period, and water depth can be made. Given a range of wave periods from 3-25 seconds, a range of wave height between 0.5 and 10 m, the water depth for which the bottom orbital velocity is equal to the limiting oscillatory velocity produced by the present piston and motor configuration can be determined. Figure 2.2 shows the limiting (minimum) water depth that bottom orbital velocities can be produced by the present system configuration as a function of wave height and wave period. Figure 2.2 uses a maximum channel oscillatory velocity of 1.2 m/s.

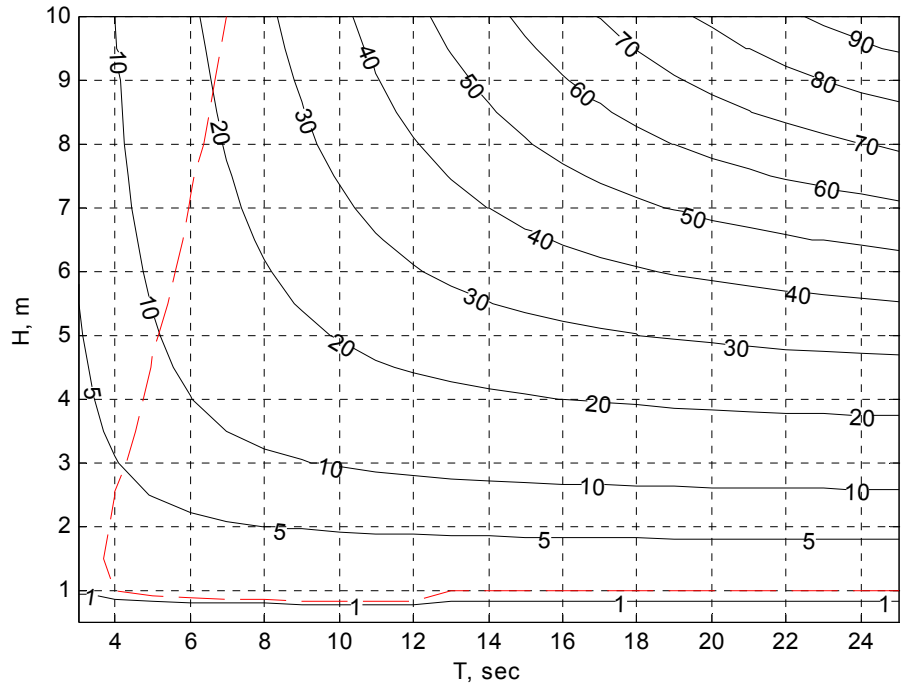

Figure 2.2. Operational limits of SEAWOLF based on linear wave theory. Provides limits of wave height, wave period, and water depth that SEAWOLF can represent within the operational limits of the motor drive and piston stroke length (V_c = 1.2 m/s). Contours are of water depth in meters. Red dashed line indicates wave-breaking limit. Conditions below and to the left of the line are unstable wave conditions and will break.

Because the bottom boundary layer in a 2 cm deep flume will be different from a free surface, the shear stresses produced in the flume will not be identical to the shear stresses produced by the surface wave and associated bottom orbital velocities. However the results shown in Figure 2.2 can be considered a first-order estimate of the limits on wave conditions that SEAWOLF can represent.

2.3 Controlled Linear Motion for Waveforms

A computer controlled stepper motor attached to a linear ball-screw drives the piston movements that create oscillating waves in the flume channel and test section (Figure 2.1a). The stepper motor makes 200 steps per revolution (1.8^{o} per step) and is part of a linear motion system that includes a ball-screw assembly with 1-inch linear travel every 4 revolutions. The maximum torque produced by the motor is 1,100 in-oz and occurs between 100-1,500 step/s. Above 1,500 step/s, the torque decreases rapidly and the motor tends to stall. Therefore, the largest stable velocity created by the pistons is approximately 1.2 m/s.

The stepper motor is computer controlled using the SMC40 Intelligent Indexer Version 1.13 software developed by Anaheim Automation. The simplest program for the controller is a trapezoidal move comprising a constant piston acceleration period, a constant rate period, and a constant deceleration period (returning to zero velocity). Dividing the trapezoid into equal sections of acceleration, constant rate, and deceleration yields the closest approximation to a half a sine wave. Figure 2.3 compares a sine wave and the trapezoid shape for a 27.5 gpm peak flow rate. The configuration for the trapezoidal move can be scaled for any motor rate and corresponding flow rate to simulate multiple wave conditions. More complex waveforms could also be simulated by

using multi-step acceleration and deceleration periods in the controller program. Section 3.2 provides details concerning linear motion configurations and their associated flow rates.

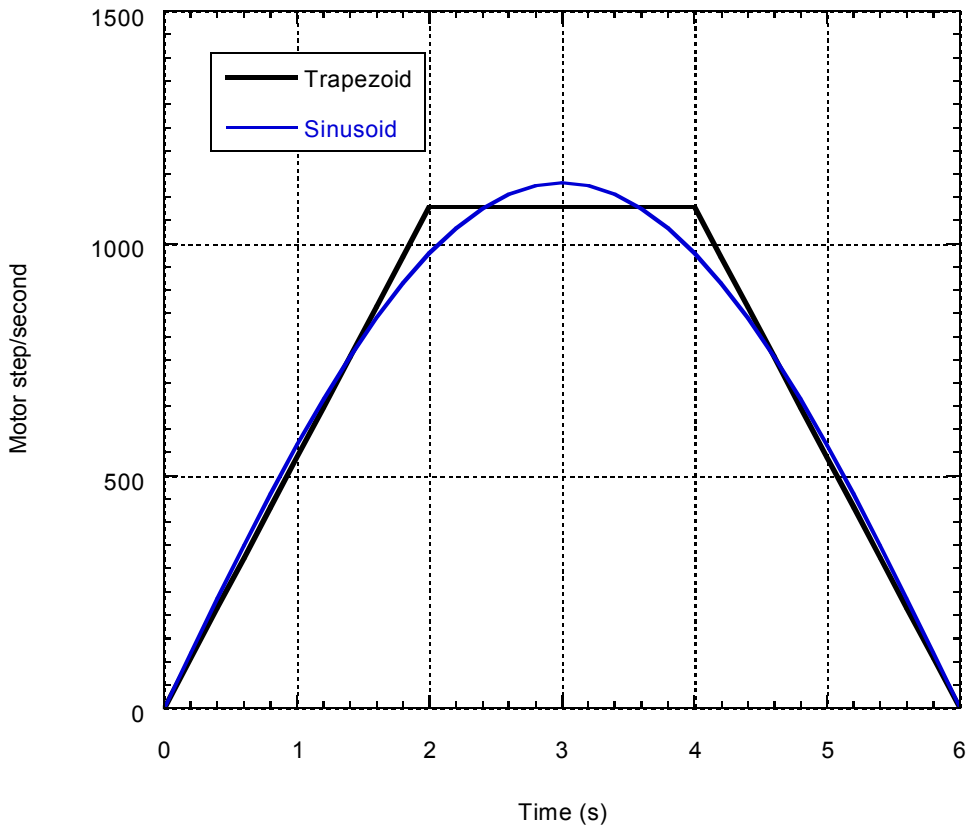

Figure 2.3: Stepper motor rate vs. time. Shown are half periods of the motor movement necessary to yield a 27.5 gpm flow rate for a sinusoidal and trapezoidal wave shape.

3.0 Results

3.1 Modeling of Flow Regime

Preliminary modeling studies investigated the relationship between flow velocities and shear stress in the flume channel under various wave/current regimes. The equations for internal channel flow in Section 2.2 are only applicable to fully developed conditions. Under oscillatory forcing, the flow is never fully developed and the relationship given by Schlichting (1979, p. 611) for hydraulically smooth internal flow underestimates the shear stress. To address undeveloped flow conditions, fine-scale numerical hydrodynamic modeling of SEAWOLF was conducted to examine the undeveloped flow conditions. The SEAWOLF numerical model was generated using Adaptive Research's Stormflow computational fluid dynamic software to simulate flow fields subject to specified initial and boundary conditions. Multiple head difference and piston movement combinations were simulated to understand flow and shear stress conditions in SEAWOLF.

The geometry of the model is identical to the flume channel shown in Figure 2.1a. The grid generated for the geometry has 200 equally spaced cells in the horizontal and 25 cells in the vertical. The vertical cells were stretched from the center of the channel by a power of 1.5 towards the top and bottom of the channel in order to simulate the boundaries in greater detail. Since the side walls are not of interest to the shear stress at the sediment/water interface, the cell resolution across the channel was limited to three and the friction on these walls was neglected.

The conditions at the inlets of the channel were user defined and submitted to the model using a subroutine. The equation describing the flow in the subroutine is

$$V = V_m \sin(\omega t) + V_{ud} \qquad (3.1)$$

V_m = maximum velocity (m/s)
V_{ud} = unidirectional velocity (m/s)

Shear stress calculations were post processed after each simulation of the transient (oscillatory) flow field. The shear stress equation used is

$$\tau = \mu \frac{\partial u}{\partial y}, \qquad (3.2)$$

u = local velocity (m/s),
μ = dynamic viscosity (kg/m-s).

For oscillatory flow, both u and τ are functions of time and may be determined at any instant during the oscillation. Shear stresses calculated for the unidirectional case only matched well with those calculated using equations (2.1) and (2.2).

Numerical results for wave periods between 5 and 15 s indicate shear stresses 75% to 125% greater at average and peak velocities than shear stresses predicted using fully developed theory. Table 3.1 compares various unidirectional and oscillatory flows and their associated maximum shear stresses. Figure 3.1 shows model results for a 22 gpm steady unidirectional flow rate coupled with a 15 gpm maximum, 15 s period oscillatory flow at the peak flow rate of 37 gpm (Table 3.1, Case 2). The shear stress for Case 2 is approximately 4.7 Pa when the flow is 37 gpm. Unidirectional, fully developed flow of 37 gpm (as found in SEDFlume) generates a wall shear stress of approximately 3.5 Pa.

Table 3.1: Comparison of shear stress for various flow conditions

Unidirectional Flow (gpm)	Maximum Oscillatory Flow* (gpm)	Total Peak Flow (gpm)	Case	Maximum Shear Stress (Pa)
15	0	15	-	0.8
0	15	15	-	1.4
22	0	22	-	1.5
37	0	37	1	3.5
22	15	37	2	4.7
15	22	37	3	7.0

*15 s period sinusoidal wave

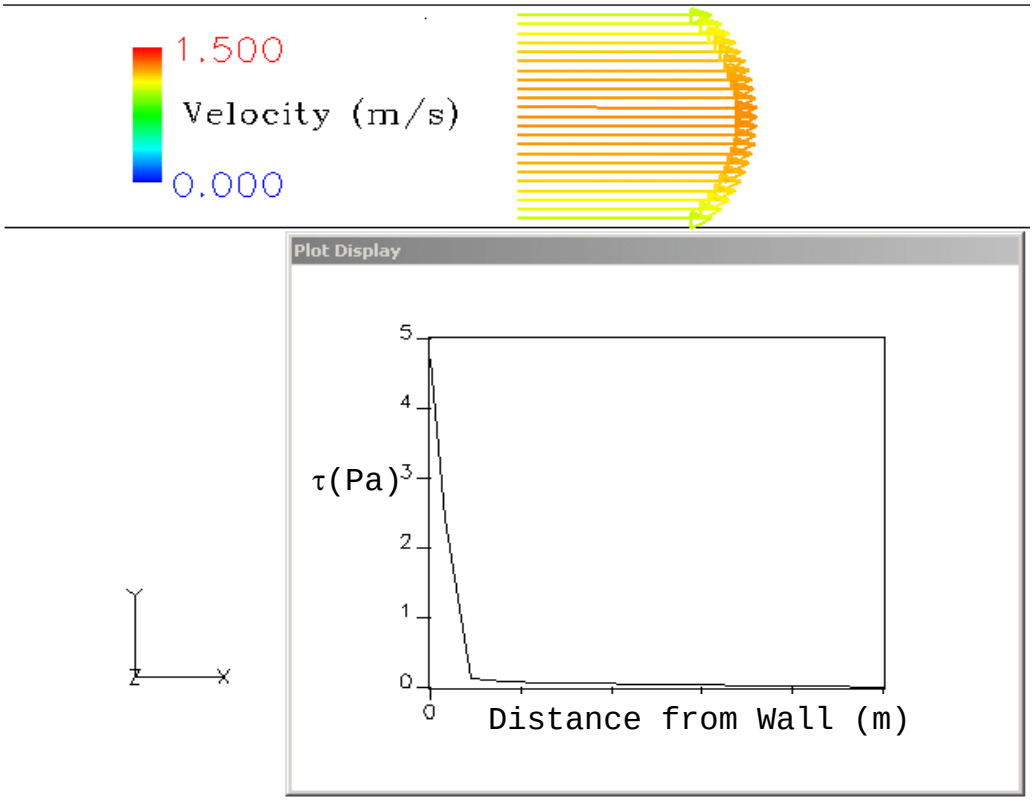

Figure 3.1: Side view of channel test section with shear stress plotted verses the distance from the channel wall where the sediment-water interface exists. Conditions are for Case 2 in Table 3.1 at the peak flow.

Interaction of unidirectional and oscillatory flows also affects shear stress (Grant and Madsen, 1976). This process is also simulated in the Stormflow simulations. The time history of shear stress for the case described in Figure 3.1 is provided in Figure 3.2.

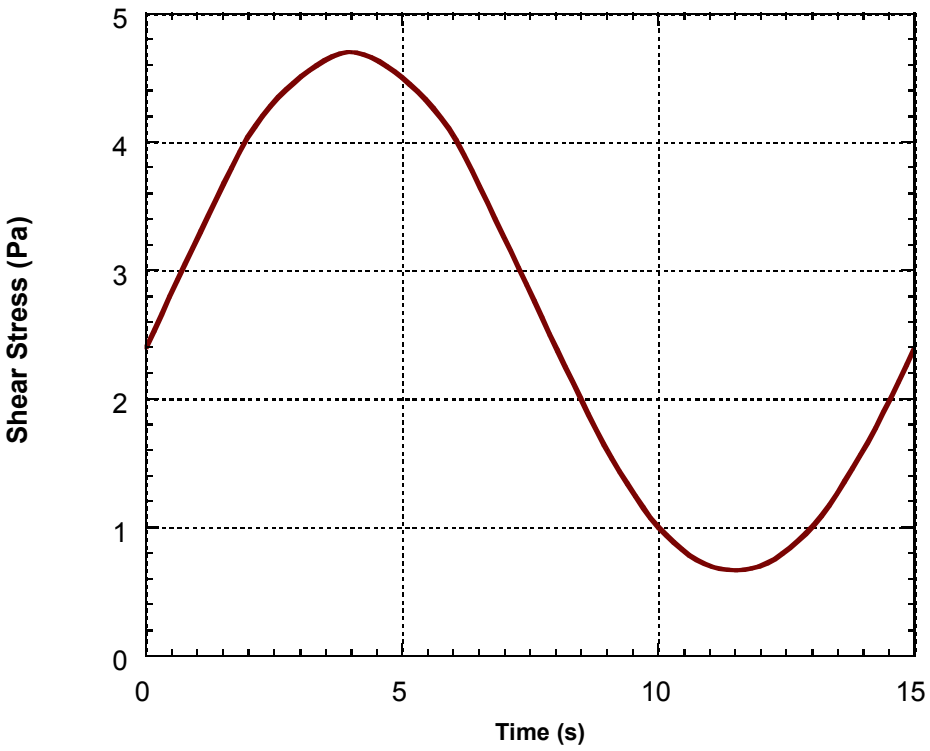

Figure 3.2: Time history of shear stress for 22 gpm unidirectional plus 15 gpm oscillatory flow with 15 s period.

Unidirectional flow rate, cycle period, piston speed, piston displacement, and trapezoid shape influence shear stress time history through a cycle. Therefore, a multi-dimensional array for wave/current regimes of interest must be based in numerical model simulations to relate shear stress to flow conditions. An example of the necessity for this is demonstrated through Table 3.1 where a 37 gpm maximum flow rate produced three

different maximum shear stresses dependent on the state of boundary layer development (Cases 1, 2, and 3). The shape of the boundary layer is a function of the specific period and amplitude for each oscillatory motion. Case 1 has 37 gpm unidirectional, fully developed, constant flow and is the lowest shear stress of the three cases shown for 37 gpm. However, Case 2 and 3 also have a maximum flow of 37 gpm, but comprise a 15 s period oscillatory flow combined with a unidirectional flow. Oscillatory Cases 2 and 3 both had greater maximum shear stresses than the unidirectional case because the boundary layer is undeveloped and smaller, with a steeper velocity gradient. Case 2 produced a significantly lower shear stress than Case 3. The larger amplitude oscillation in Case 3 (±22 gpm) had the largest maximum shear stress because it has the most undeveloped boundary layer of all three cases. However, the time history of shear stress for the two oscillatory cases varies and has shear stresses lower than the constant shear stress at 37 gpm from unidirectional flow only. For example, the shear stress for Case 3 is zero at two instants during the wave period because the flow reverses direction.

3.2 Flow Tests

Several experiments were conducted in the oscillatory flume to validate design parameters and test equipment. A DeltaForce^{TM} magnetic flow meter attached directly to one end of the channel was used to provide real-time measurements of flow conditions. Wave shape variations with peak flow rates of 40 gpm were studied.

Several flow conditions were tested where motor speeds and valve configurations were altered. Figure 3.3a-h shows flow rates for these oscillatory conditions. All motor movements were trapezoidal approximations of a half sine wave. Sinusoidal curve fits (red line) are provided in each figure. Each pair of figures (3.3a-b, 3.3c-d, 3.3e-f, 3.3g-h)

demonstrates the same motor movement for valves fully open and valves completely closed conditions. The tests demonstrate that the each motor-piston movement closely simulates sinusoidal flow rates and velocities under both valve open and valve closed conditions. In some cases, there appeared to be slightly lower velocities in the first quarter (acceleration) of the wave cycle compared to the second quarter (deceleration). This may have been due to the smaller diameter pipe (1.5 in) in the flow meter attached at on end of the channel compared to the 2 in diameter elsewhere in the system. The smaller diameter in the flow meter could cause more head loss during the accelerated flow compared to the decelerated flow. If further testing shows this effect to be significant and consistent, it could be corrected by using a valve on the opposite side of the channel to equilibrate any head loss associated with the flow meter. In addition, once the flow meter is used to establish flow characteristics for specific piston motions and tank configurations, it could be removed.

Valve closed cases generate 5-10 gpm greater peak flow rates compared to valve open cases under identical motor-piston movements for the conditions tested. This indicates that the flow impulse is significantly redirected to the open tanks when the valves are open, although the oscillatory flow in the valve-open case remains sinusoidal. When the valves are closed, the flow cannot be redirected to the tanks and must travel through the flume channel. Flow meter measurements for the valve closed cases are consistent with calculations for the volume of fluid displaced by the piston movement (Section 2.2.2). The sole exception is for the case shown in Figure 3.3a where the flow meter value is approximately 20% greater than piston displacement estimates.

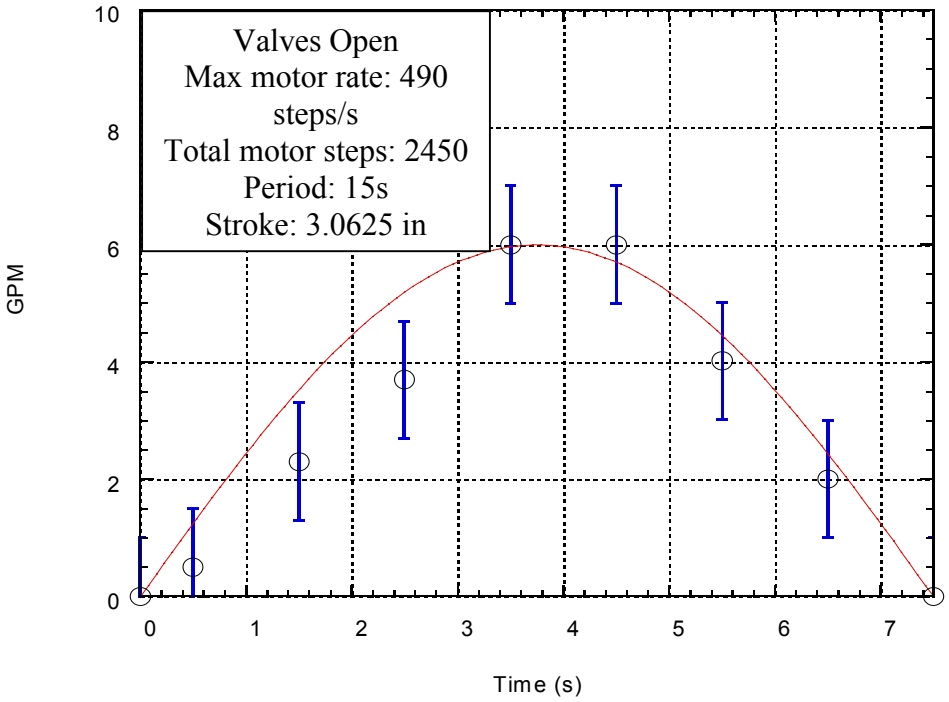

Figure 3.3a: Valve open, 6.0 max gpm (0.185 m/s).

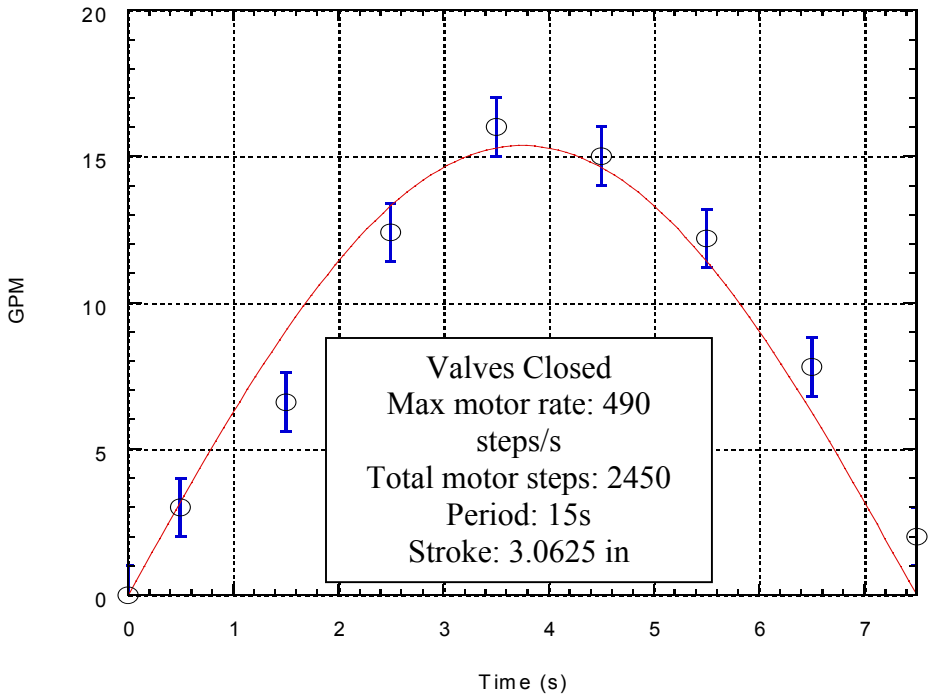

Figure 3.3b: Valve closed, 15.0 max gpm (0.45 m/s).

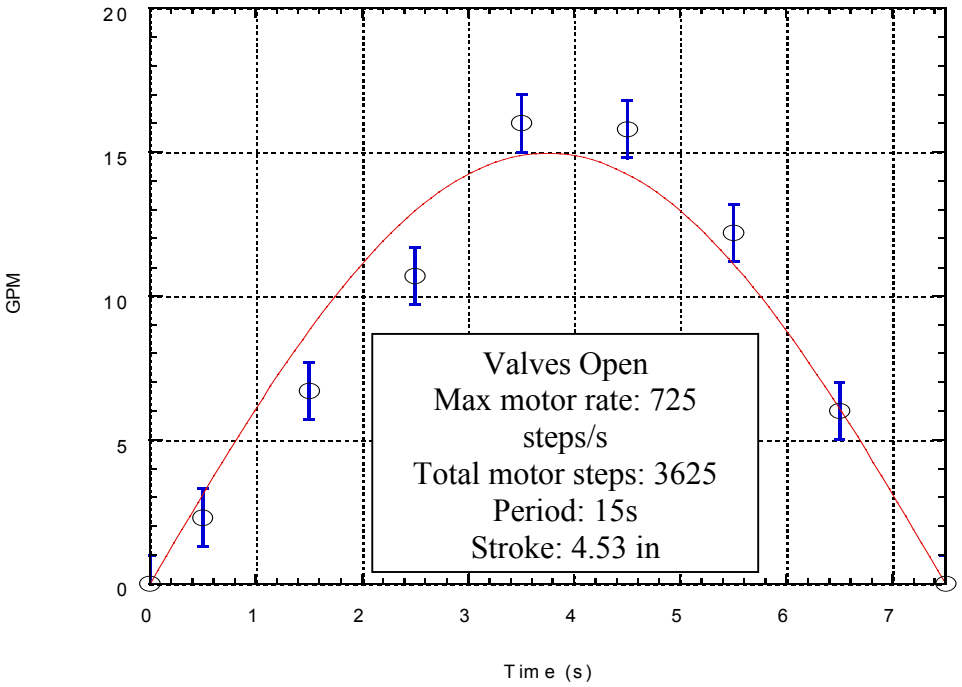

Figure 3.3c: Valve open, 15.0 max gpm (0.45 m/s).

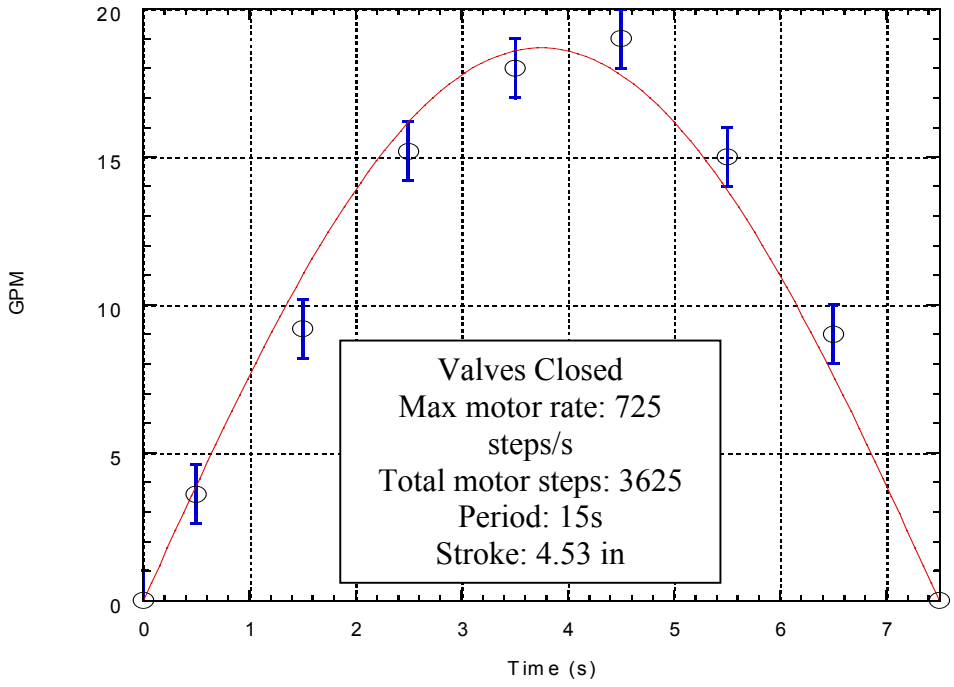

Figure 3.3d: Valve closed, 18.5 max gpm (0.55 m/s).

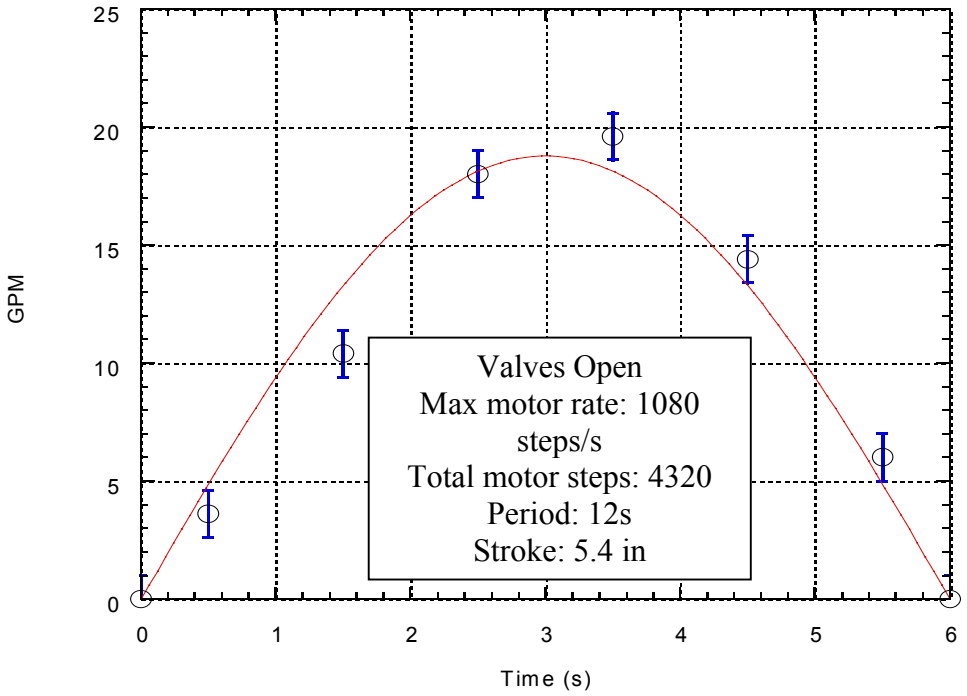

Figure 3.3e: Valve open, 18.3 max gpm (0.55 m/s).

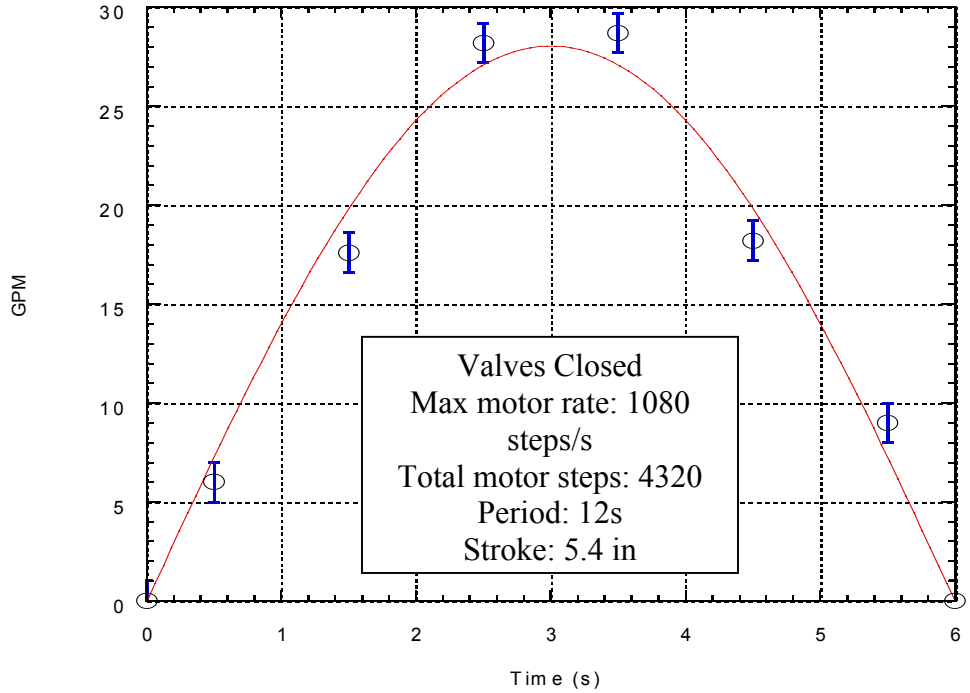

Figure 3.3f: Valve closed, 27.5 max gpm (0.82 m/s).

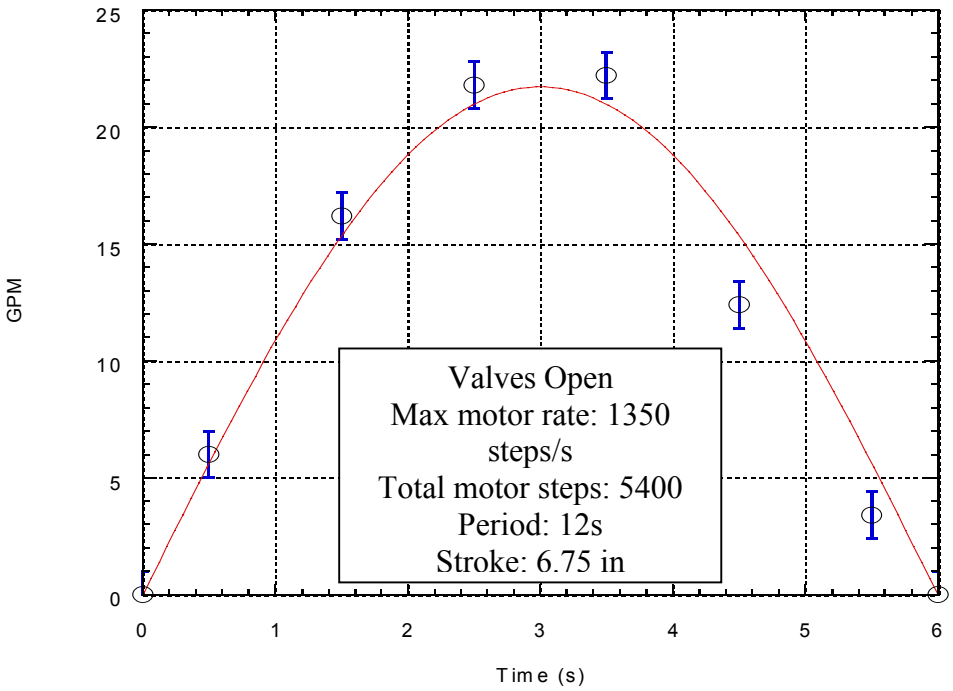

Figure 3.3g: Valve open, 22.0 max gpm (0.65 m/s).

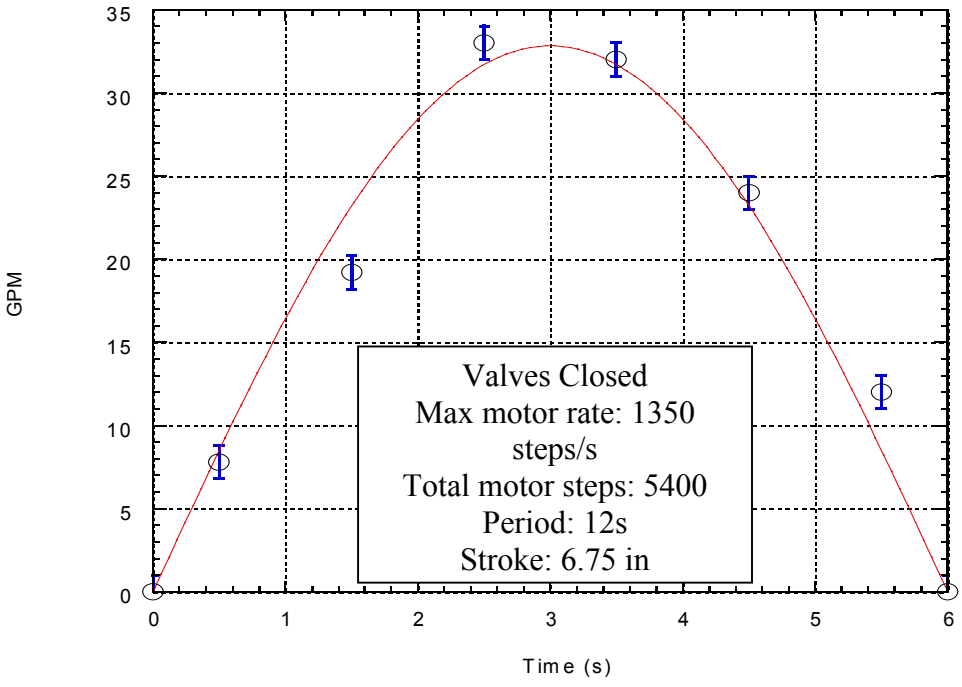

Figure 3.3h: Valve closed, 33.0 max gpm (0.99 m/s).

Additional testing was performed for combined oscillatory and unidirectional flow. Figure 3.4 shows the results for a 22 gpm unidirectional flow (Δh=0.3 m for valve open case) superimposed upon a 15 gpm peak, sinusoidal, 15 s period oscillating flow. Experimental results correlate well with the numerical model described in Section 3.1. The combined unidirectional/oscillatory flow shown in Figure 3.4 has the same motor motion as the case described in Figure 3.3c (725 steps/s maximum motor rate and 3625 motor steps per stroke). Measurements indicate that the sinusoidal oscillatory flow generated by the pistons was maintained in the presence of the unidirectional flow. The maximum flow rate was 36 gpm (approximately 22 gpm +15 gpm) and a minimum 8 gpm (approximately 22 gpm – 15 gpm).

Figure 3.4: Maximum motor rate of 725 step/s with a total of 3625 motor steps. Valves are open with 22 gpm of superimposed unidirectional flow.

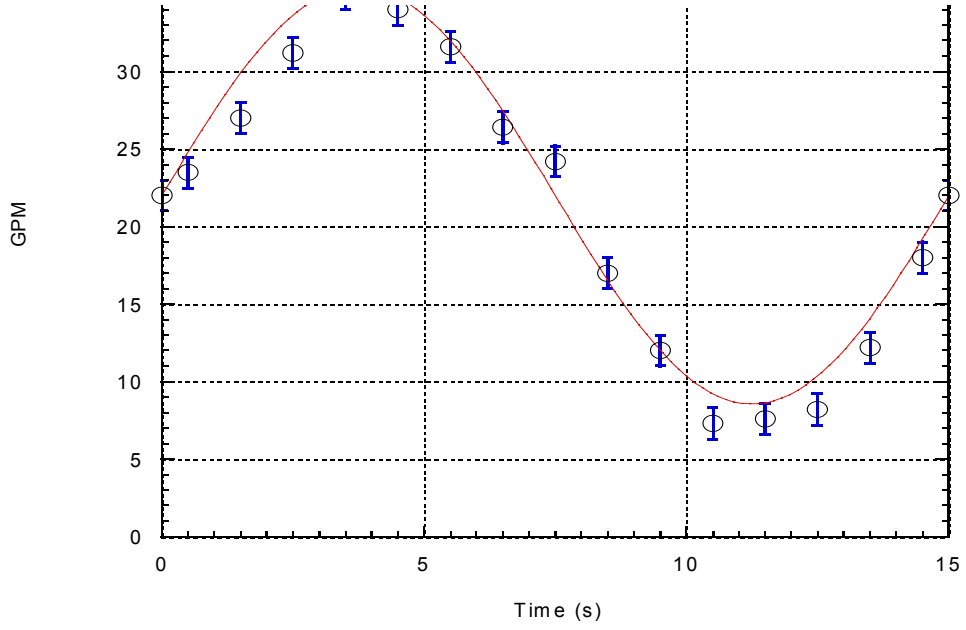

3.3 Oscillatory Erosion Tests

3.3.1 Quartz Sand Tests

Erosion tests were performed on a 310 μm quartz sand that has been tested extensively in the unidirectional SEDFlume (McNeil et al., 1996). Tests were performed with the valves open for the piston moves described in Figure 3.3a,c,e,g. Table 3.2 shows the SEAWOLF experimental results for these piston moves. Erosion rate is measured as the operator controls upward movement of the core over the duration of the experiment. It should be noted that erosion rates measured in SEDFlume are consistent with known erosion rates for sands (Roberts et al., 1998) under multiple shear stress and grain size conditions.

Table 3.2: Erosion for 310 μm quartz sand

Average Flow (gpm)	Maximum Flow (gpm)	Reference Figure	Erosion Rate (cm/s)	Effective Shear Stress for Wave (Pa)
3.27	6.0	3.3a	~0	-
9.3	15.0	3.3c	0.006	0.7
12.0	18.3	3.3e	0.0183	1.0
13.7	22.0	3.3g	0.05	1.5

The equation describing the erosion rate as a function of shear stress (Jepsen et al., 1997) is

$$E = A\rho^m \tau^n \qquad (3.3)$$

where A =1.7x10^{-2}, m= 0, and n=2.7 for 310 μm quartz (Roberts and Jepsen, 2001). Solving equation (3.3) for shear stress, τ, and substituting the values in Table 3.2 for erosion rate, E, yields an effective shear stress for the wave motion. Effective shear stress in Table 3.2 is the shear stress from the unidirectional SEDFlume that induces the same erosion rate in SEAWOLF.

3.3.2 Natural Sediment Tests

Experiments were also performed with sediments from the Canaveral Ocean Dredged Material Disposal Site for the combined unidirectional and oscillatory flow case shown in Figure 3.4. The same sediments (site CDS-2) were tested extensively using the unidirectional SEDFlume (Jepsen et al., 2001). The sediments were 63% sand and 37% silt with a median grain size of 92 μm. The constants derived from the unidirectional tests for equation (3.3) are A =1.22x10^{10}, m= -66.8, and n=2.71. The erosion rate measured for the superimposed oscillatory and linear flow conditions of Figure 3.4 and Table 3.1 Case 2 was 0.00133 cm/s. With this erosion rate, equation (3.3) yields an effective shear stress of 2.4 Pa. According to equations (2.1) and (2.2) the shear stress in SEAWOLF for a 22 gpm unidirectional, fully developed flow rate is approximately 1.4 Pa (Table 3.1). Clearly undeveloped oscillatory flows generate significantly higher erosion rates and effective shear stresses than the equivalent unidirectional, fully developed flow rates. The effective shear stress is higher for the oscillatory case because either the flow is not fully developed, the maximum flow (37 gpm) and related shear stress (~4.7 Pa from modeling results) is the controlling factor, or oscillatory flow may weaken the sediment surface more than a constant, unidirectional flow.

3.4 Effective Shear Stress

In summary, the effective shear stress for unsteady wave/current conditions is used to represent an equivalent erosion rate for a unidirectional, fully developed flow. Erosion rate is generally a function of shear stress to a power greater than one ($E \sim \tau^{>1}$). It is also probable that a portion of the wave period may include shear stress less than the critical shear stress for initiation of erosion. Therefore, effective shear stress is not the same as average shear stress or maximum shear stress for the wave/current condition, but a function of shear stress time history and critical shear stress. Nevertheless, effective shear stress is the most useful description for bulk erosion measurements because it is operationally impossible to measure cohesive sediment erosion rates for small time periods within a wave period. The effective shear stress is also the simplest and most useful measurement for model input. To determine shear stresses at discrete times within the wave period requires intense numerical computations that are beyond the capacity of most large domain sediment transport models.

There exists an extensive library of sediments in which the constants for equation (3.3) have been determined under unidirectional flow (Roberts et al., 1998; Jepsen et al., 1997; Jepsen et al., 2001). A general relationship between various waveforms and effective shear stresses could be developed through further experiments with more quartz sands and other natural sediments with well known erosion properties for unidirectional, fully developed flow. These experiments coupled with modeling efforts, would create a much-improved understanding of erosion processes of combined wave and current regimes.

At present, effective shear stress can only be calculated for sediments with known unidirectional, fully developed flow generated erosion rates. Effective shear stress is also specific to both sediment properties and wave/current conditions. Additional SEAWOLF erosion tests and modeling will develop relationships that describe the influence of wave/current conditions on effective shear stress.

4.0 Conclusions

A new erosion flume, SEAWOLF, has been developed by SNL. SEAWOLF combines oscillatory and linear flow to measure erosion rates and erosion variation with depth. Motor and controller software is used to generate motor moves that simulate waveforms. Numerical modeling simulations were conducted using various flow oscillation period and magnitudes combined with unidirectional current regimes. The oscillatory flow combinations represented a variety of wave conditions. With SEAWOLF, oscillatory flow variations successfully created shear stress up to 10 Pa. The addition of unidirectional flow superimposed upon the oscillatory flow generated shear stresses greater than 12 Pa.

Flow was measured and erosion tests were performed in SEAWOLF with both quartz sand and a natural sediment that were well classified in unidirectional erosion tests. Both modeling and erosion results showed that the shear stress is much higher in the undeveloped, oscillatory flow regime than for fully developed, unidirectional flow at the same flow rate. Results demonstrate the utility of the SEAWOLF for producing combined oscillatory and unidirectional flows as a modification to a well-established framework for measuring erosion for unidirectional, steady flows.

The erosion rates measured in SEAWOLF over a wave form can be estimated by an effective shear stress that is related to the equivalent erosion rate from unidirectional tests. However, to develop a robust operation protocol and improve the understanding of the erosion processes, more studies must be conducted with a variety of sands and sediments.

5.0 References

Grant, W.D. and O.S. Madsen, 1979. Combined wave and current interaction with a rough bottom. J. Geophys. Res., 84(C4), 1797-1808.

Jepsen, R., J. Roberts, and W. Lick, 1997. Effects of bulk density on sediment erosion rates, *Water, Air, and Soil Pollution*. Vol. 99, 21-31.

Jepsen, R., J. Roberts, A. Lucero, and M. Chapin, 2001. Canaveral ODMDS Dredged Material Erosion Rate Analysis. SAND2001-1989. Sandia National Labs, Albuquerque, New Mexico, 87185.

McNeil, J., C. Taylor, and W. Lick, 1996. Measurements of Erosion of Undisturbed Bottom Sediments with Depth. *Journal of Hydraulic Engineering*. 122(6), 316-324.

Roberts, J., R. Jepsen, D. Gotthard, and W. Lick, 1998. Effects of particle size and bulk density on erosion of quartz particles. *Journal of Hydraulic Engineering*. 124(12), 1261-1267.

Roberts, J. and R. Jepsen, 2001. Separation of Bedload and Suspended Load with Modified High Shear Stress Flume. SAND2001-2162. Sandia National Labs, Albuquerque, New Mexico, 87185.

Schlichting, H., 1979. *Boundary-Layer Theory*. Seventh ed, McGraw-Hill. pp.814.

DISTRIBUTION

External

Richard Langford
Department of Geological Sciences
University of Texas at El Paso
El Paso, TX 79968-0555

US Army Corps of Engineers
Coastal and Hydraulics Laboratory
CEWES-CC-C
3909 Halls Ferry Rd
Vicksburg, MS 39180
Attn: Joseph Gailani

Rong Kuo
International Boundary & Water Commission
4171 N. Mesa C-310
El Paso, TX 79902

Manuel Rubio, Jr.
International Boundary and Water Commission
4171 N. Mesa C-310
El Paso, TX 79902-1441

Paul Tashjian
Department of the Interior
US FISH AND WILDLIFE SERVICE
P.O. Box 1306
Albuquerque, NM 87103-1306

Thanos N. Papanicolaou
Washington State University
PO Box 642910
Pullman, WA 99164-2910

Jerry Wall
U.S. Department of the Interior
Bureau of Land Management
435 Montano N.E.
Albuquerque, NM 87107

Craig Jones
Woods Hole Group
1167 Oddstad Dr.
Redwood City, CA 94063

U.S. Army Corps of Engineers
Coastal and Hydraulics Laboratory
CEWES-CC-D
3909 Halls Ferry Rd
Vicksburg, MS 39180
Attn: Jarrel Smith

John R. Gray
U.S. Department of the Interior
U.S. Geological Survey
12201 Sunrise Valley Drive
415 National Center
Reston, VA 20192

John W. Longworth
Interstate Streams Commission
P.O. Box 25102
Santa Fe, NM 87504-5102

Pravi Shrestha
HydroQual, Inc.
One Lethbridge Plaza
Mahwah, NJ 07430

Rodrick D. Lentz
U.S. Department of Agriculture
3793 N. 3600 E.
Kimberly, ID 83341-5076

Christopher J. McArthur, P.E.
U.S. EPA Region 4
Wetlands, Coastal & NonPoint
Source Branch
61 Forsyth Street, S.W.
Atlanta, GA 30303

Kirk Ziegler
Quantitative Environmental Analysis, LLC
305 West Grand Avenue
Montvale, NJ 07645

Joseph V. DePinto
Senior Scientist
Limno-Tech, Inc.
501 Avis Drive
Ann Arbor, MI 48108

Wilbert J. Lick
Dept. of Mechanical & Environmental Engineering
University of California, Santa Barbara
Santa Barbara, CA 93106-5070

Internal

MS	Org.	
0701	6100	W. Cieslak
0701	6100	P. Davies
0735	6115	D. Thomas
0735	6115	E. Webb
0771	6800	D.R. Anderson
1395	6820	P.E. Shoemaker
1395	6822	F.D. Hansen
1395	6822	R. Jepsen (3)
1395	6822	J. Roberts (3)
1395	6820	F.C. Allan (6)
0755	6251	M. Hightower
9018	8495-1	Central Technical Files
0899	9616	Technical Library (2)
0612	9612	Review and Approval Desk for DOE/OSTI